COMPARISON OF CALCULATIONS OF FLOW PAST A CURVED HILL USING RECTANGULAR AND BOUNDARY-FITTED GRIDS

Sankara N.VENGADESAN[1] and Akihiko NAKAYAMA[2]

[1]Research Associate, Division of Global Development Science, Graduate School of Science and Technology, Kobe University
[2]Professor, Division of Global Development Science, Graduate School of Science and Technology, Kobe University
(1-1, Rokkodai Nada, Kobe 657-8501)

Flows past curved hills have been computed by the numerical method based on the boundary-fitted coordinate and the Cartesian coordinates to investigate the difference and demerits of two different approaches. Calculation results at high Reynolds number laminar flow using central difference scheme for convective terms lead to pressure oscillation when the geometry is approximated by rectangular coordinate and results in stable calculation when the geometry is approximated by boundary-fitted grid or by using upwind scheme. LES calculation results with upwind scheme at higher *Re* predicts similar trend in both grid systems. For calculations of flow past complex boundary, where generating boundary-fitted grid is almost impossible or difficult, rectangular coordinate approximation can be good alternative.

Key Words: finite difference methods, complex boundary, boundary-fitted and rectangular grid

1. INTRODUCTION

Recent advancements of both computers and numerical methods have made it possible to calculate turbulent flows of various kinds. Calculation of complex three-dimensional flows in natural enviornment and in complex machineries is becoming within the range of readily accessible computers[1),2)]. One of the tasks yet to be accomplished in hydraulic and atmospheric applications is to device an effective way of representing complex natural topography. Various methods are developed and tested; the present authors have developed a few different ways of dealing with complex boundaries. First method is to use the curved coordinate system that follows the shape of the boundary. Once a good grid is generated, boundary conditions are set at exact locations and the flow over it can be calculated with relative ease. One problem with this method is that when the boundary becomes irregular or not smooth, it becomes impossible to generate a grid. In such a situation, usually, one has to resort to other methods like a multi-block approach and local refinement and generating a grid with good quality becomes difficult. Furthermore, transformation of the governing equations results in a complex system of equations with many geometric parameters implying high computational overhead. The second method is to use the rectangular grid in Cartesian coordinates[3),4),5)]. In this method, generation of grid is trivial and arbitrary shapes can be represented. Because of these advantages many new methods of using rectangular grids for complex shapes with various boundary treatments are proposed[6),7)]. One disadvantage of using the rectangular grid for arbitrary shape is that either the position of the boundary becomes approximate or the boundary conditions are applied at interpolated points.

In computing flows over complex topography or similar complex geometry, it will help if relative performance and accuracies are known for these different methods. In the present work, we compare calculation of flow past smooth curved hills with small and unfixed flow separation using both boundary-fitted coordinate and the Cartesian coordinates. First, basic performance of each method is examined in low-Reynolds number laminar flow, and then accuracies and stability are examined at high Reynolds numbers. Then the methods are evaluated when applied to large-eddy simulation (LES) of higher Reynolds number turbulent flow in the same geometrical region. The test calculations for the turbulent case are performed for the cases in which detailed experimental data are available.

2. NUMERICAL METHODS FOR RECTANGULAR GRID (RC)

Here the methods using the rectangular grid are described. They are for computing the flow of incompressible fluid of density ρ and kinematic viscosity ν. The governing equations are the

conservation equations for mass and momentum

$$\frac{\partial u_i}{\partial x_i} = 0, \tag{1}$$

$$\frac{\partial u_i}{\partial t} + u_i \frac{\partial u_j}{\partial x_i} = -\frac{1}{\rho}\frac{\partial p}{\partial x_i} + \nu \frac{\partial^2 u_i}{\partial x_j \partial x_j}. \tag{2}$$

Here u_i is the component of the velocity vector in the Cartesian coordinate x_i. We also use the notation (x,y,z) for (x_1,x_2,x_3) and (u,v,w) for (u_1,u_2,u_3). These equations are discretized, with variables arranged in staggered system to apply conveniently the pressure-coupling algorithm. Fig.1 shows the grid arrangement and the points where the boundary conditions are applied. Discretization of convective terms are done by a third order upwind differencing, UTOPIA or by conservative second order central difference scheme[8]. Viscous terms are discretized by second-order accurate central differencing scheme. HSMAC iteration procedure is used for calculating pressure. Time advancing of the momentum equations is done by a second-order accurate explicit, Adams-Bashforth method. Performance of the code for laminar and turbulent flow past a bluff body and turbulent flow over curved geometry have been assessed earlier[9),10)].

3. NUMERICAL METHODS FOR BOUNDARY-FITTED GRID (BFC)

In order to solve the same incompressible flows in boundary-fitted grid, equations (1) and (2) are transformed in general coordinates and they are given as

$$\frac{\partial U_m}{\partial \xi_m} = 0, \tag{3}$$

$$J^{-1}\frac{\partial u_i}{\partial t} + \frac{\partial}{\partial \xi_m}\{U_m u_i\} = -\frac{\partial}{\partial \xi_m}\left\{A_i^m \frac{p}{\rho} - \nu G^{mn}\frac{\partial u_i}{\partial \xi_n} - \nu J^{-1}\frac{\partial \xi_m}{\partial x_j}\frac{\partial \xi_n}{\partial x_i}\frac{\partial u_j}{\partial \xi_n}\right\}. \tag{4}$$

where

$$J^{-1} = \det\left(\frac{\partial x_i}{\partial \xi_j}\right); \quad A_i^m = J^{-1}\frac{\partial \xi_m}{\partial x_i}; \quad G^{mn} = J^{-1}\frac{\partial \xi_m}{\partial x_j}\frac{\partial \xi_n}{\partial x_j}; \quad U_m = A_m^j u_j. \tag{5}$$

Here x_i is the Cartesian coordinate fixed in the physical space, and ξ_m is the general coordinate used in the computation. J is the Jacobian of the transformation matrix from x_i to ξ_m and U_m is the contravariant component of the velocity vector multiplied by J^{-1}, which represents the volume flux in the direction perpendicular to the surface ξ_m = constant. For laminar flow, the last term will disappear and for turbulent flow, which is solved assuming the eddy-viscosity formulation for the subgrid scale stresses, the eddy viscosity ν_G is added to ν as explained in the next section.

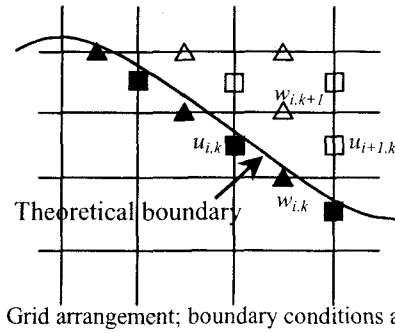

Fig.1. Grid arrangement; boundary conditions are enforced at locations marked by filled symbols

Discretization in BFC using staggered variable arrangement is very insufficient involving complex coding and additional computational loads. Therefore the method based on the colocated variables is used here. The discretization procedure follows the fractional-step method with the Crank-Nicolson implicit differencing for the diagonal elements of the viscous terms and the second-order Adams-Bashforth scheme for the off-diagonal viscous terms and the advective terms. The spatial differencing of the nonlinear advective terms is done by either the second-order consistent scheme[11)] or UTOPIA and the rest are done by the second-order central differencing scheme. Other details of the BFC code and validation for benchmark problems are the same as Ref.12.

4. SUBGRID STRESS MODEL FOR LES

When the above methods of flow solution are used in Large Eddy simulation (LES) of turbulent flows, all variables in the equations are the respective filtered quantities of the instantaneous flow. The additional stress called subgrid-scale stress R_{ij} appears in the momentum equations. If it is modeled by conventional eddy-viscosity model, which is given as,

$$R_{ij} = \frac{2}{3}k_s\delta_{ij} - 2\nu_G S_{ij} \tag{6}$$

where, k_s is the subgrid turbulent kinetic energy, δ_{ij} is the Kronecker delta, ν_G is the subgrid eddy viscosity and S_{ij} is the strain tensor, then ν_G needs to be added ν in the momentum equations. ν_G is modeled by the Smagorinsky model

$$\nu_G=(C_S\Delta)^2\left[\frac{\partial u_i}{\partial x_j}\left(\frac{\partial u_i}{\partial x_j}+\frac{\partial u_j}{\partial x_i}\right)\right]^{1/2} \quad (7)$$

where, Δ is the grid size defined by the geometric average of the grid spacings in three directions, $(\Delta x_1 \Delta x_2 \Delta x_3)^{1/3}$, u_i is now the spatially filtered velocity. C_S is Smagorinsky constant, which is chosen as 0.13. In the case of BFC, coordinate transformed equations of (6) and (7) are used.

5. TEST FLOW PAST A CURVED HILL

The flow configuration considered shown in Fig.2 is that past a model isolated hill. It is a smooth two-dimensional topography, defined by an analytical expression $\frac{z_G}{H}=\frac{1}{1+(x/nH)^4}$, where z_G is the elevation of the ground at horizontal position x, and H is the height of the hill and x is the horizontal distance from the center of the hill. The steepness of the hill is determined by the value of n. For n=2.8, the largest slope angle is 20 degrees and the flow in this case contains a small separate bubble at low Reynolds numbers. For n=2.3, the largest slope is 25 degrees and the flow is considerably different with larger flow separation. These are the two test cases used for the present comparative test runs.

(1) Computational domain and grid

The computational region covers the test flow shown in Fig.2. The computational domain extends from about 8.5H upstream and 14H downstream of the hill of 25 degrees. For the hill with maximum slope angle of 20 degrees, it covers the region from -10.5H to 17H. The calculation domain extends 7H in the cross stream-wise and 4H in the spanwise directions. In the streamwise direction, points are closely spaced within 4H on either side from the hill summit. In the cross stream-wise direction, the first point from the ground is placed at 0.03H near the bottom of the wall, stretched up to 0.5H and then compressed up to 1.5H and then placed non-uniformly until the top boundary. In the spanwise direction in either grid system, grids are uniformly spaced. The total grid size is 128x21x61 and 140x21x61 respectively for 25-degree and 20-degree slope hills.

In the case of BFC, the grid is generated by transforming the physical space on the rectangular computational space by an elliptic equation and generated coordinates fit the actual boundary. Calculation domain, distance of the first grid point from the ground and grid size is the same as that of in RC.

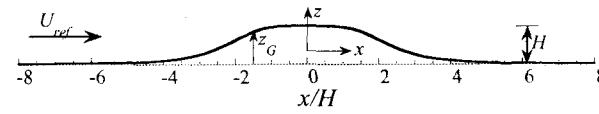

Fig. 2. Flow configuration

(2) Calculation cases

Table 1 gives the list of cases and keys used for laminar flow calculation. Reynolds number Re, is defined by the oncoming velocity U_{ref} and maximum hill height H. For turbulent flow condition, LES calculations are performed for the maximum slope of 25 degrees hill only, for the Reynolds number of 13,000, and the results are compared with available experimental data[13].

(3) Boundary conditions

Boundary conditions are enforced at inflow, downstream, top and bottom boundaries. Periodic conditions are enforced for the spanwise direction. Slip conditions on the top boundary and nonslip boundary conditions on the ground surface are applied. At downstream, radiation boundary conditions are used. At the inflow plane, uniform flow and experimental mean velocity profile available at the nearest streamwise station is given for laminar and turbulent cases, respectively. For the turbulent flow case, the nonslip condition on the ground surface may not be appropriate since the viscous sublayer is not quite resolved by the present grids. But for examining the general numerical schemes, the nonslip condition will provide a better basis for comparison.

Table 1. Calculation cases details for laminar flow condition

Maximum slope angle	*Re*	Grid arrangement	Key used
20	100	RC	H201R
		BFC	I1201B
25	100	RC	H251R
		BFC	H251B
	500	RC	H255R
		BFC	H255B

6. RESULTS AND DISCUSSION

(1) Comparison in calculation of laminar flow

First, laminar calculations are performed by both RC and BFC for flow past the hill of maximum slope angle of 25 degrees at low Reynolds number of 100 in order to verify the basic numerical procedures. Then calculations at higher Reynolds number of 500 are performed. There is no exact solution for flows of this type and these cases are run to assure that the basic methods are correct. For

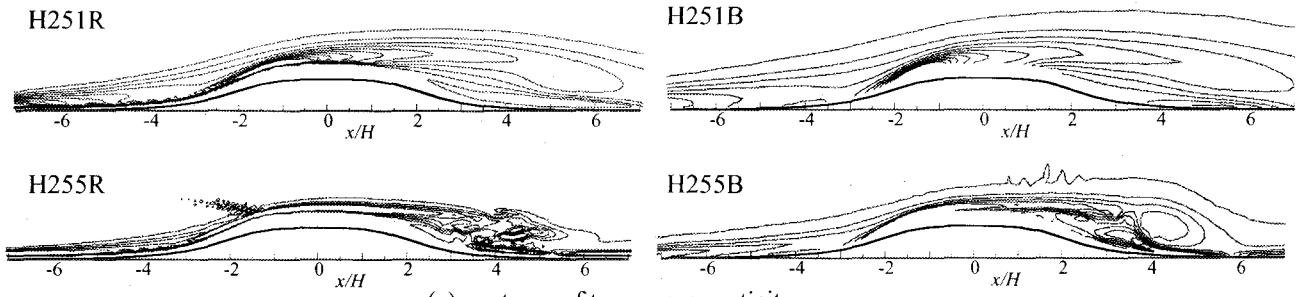

(a) contours of transverse vorticity

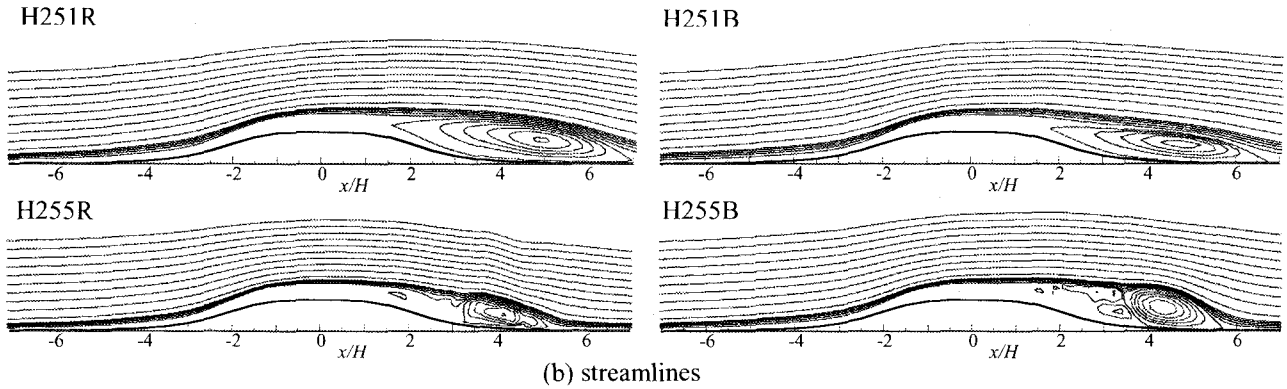

(b) streamlines

Fig. 3. Calculation results for laminar flow past hill of maximum slope of 25 degrees

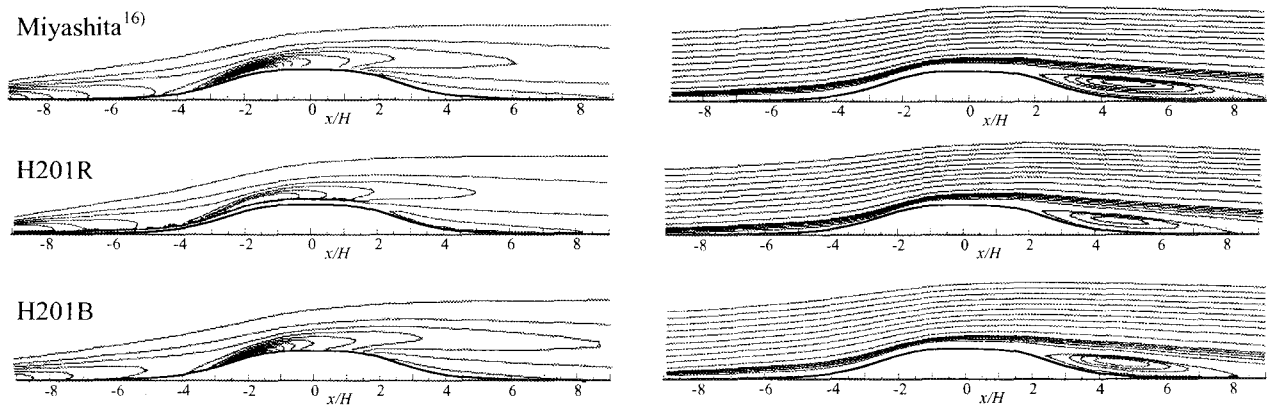

Fig 4(a) Contours of transverse vorticity

Fig 4(b) Streamlines

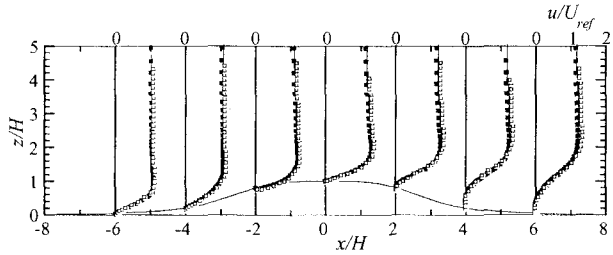

(c) Profiles of streamwise velocity; solid line - Miyashita[16)], filled square – H201R, open square – H201B

Fig. 4. Calculation results for laminar flow past hill with maximum slope angle of 20 degrees

all these cases, convective terms are discretized by second-order conservative schemes. Calculations are run with non-dimensional time increment of Δt=0.001H/U_{ref} and the results are compared at the same non-dimensional time T=40H/U_{ref}. The calculated mean-flow spanwise vorticity distribution and streamlines by RC and BFC are shown in Fig.3.

At low Re=100, results calculated by both grid systems for all the cases agree well with each other.

For higher Reynolds number of 500, we see differences in the calculated results. Small oscillations appear in the plot of spanwise vorticity calculated by RC grid. It has been pointed out[14),15)] in the calculation of flow past a bluff body similar oscillation appears also, when the cell Reynolds number becomes large and the central differencing is used for convective terms. This phenomenon can be suppressed by using an upwind differencing, which appears to be necessary for stable calculation of turbulent flows at much higher Reynolds numbers when performed on Cartesian coordinates.

In order to validate the numerical methods with UTOPIA scheme, which is known to introduce numerical viscosity, calculations are performed for the hill with maximum slope angle of 20 degrees at Re=100, and compared with numerical calculation

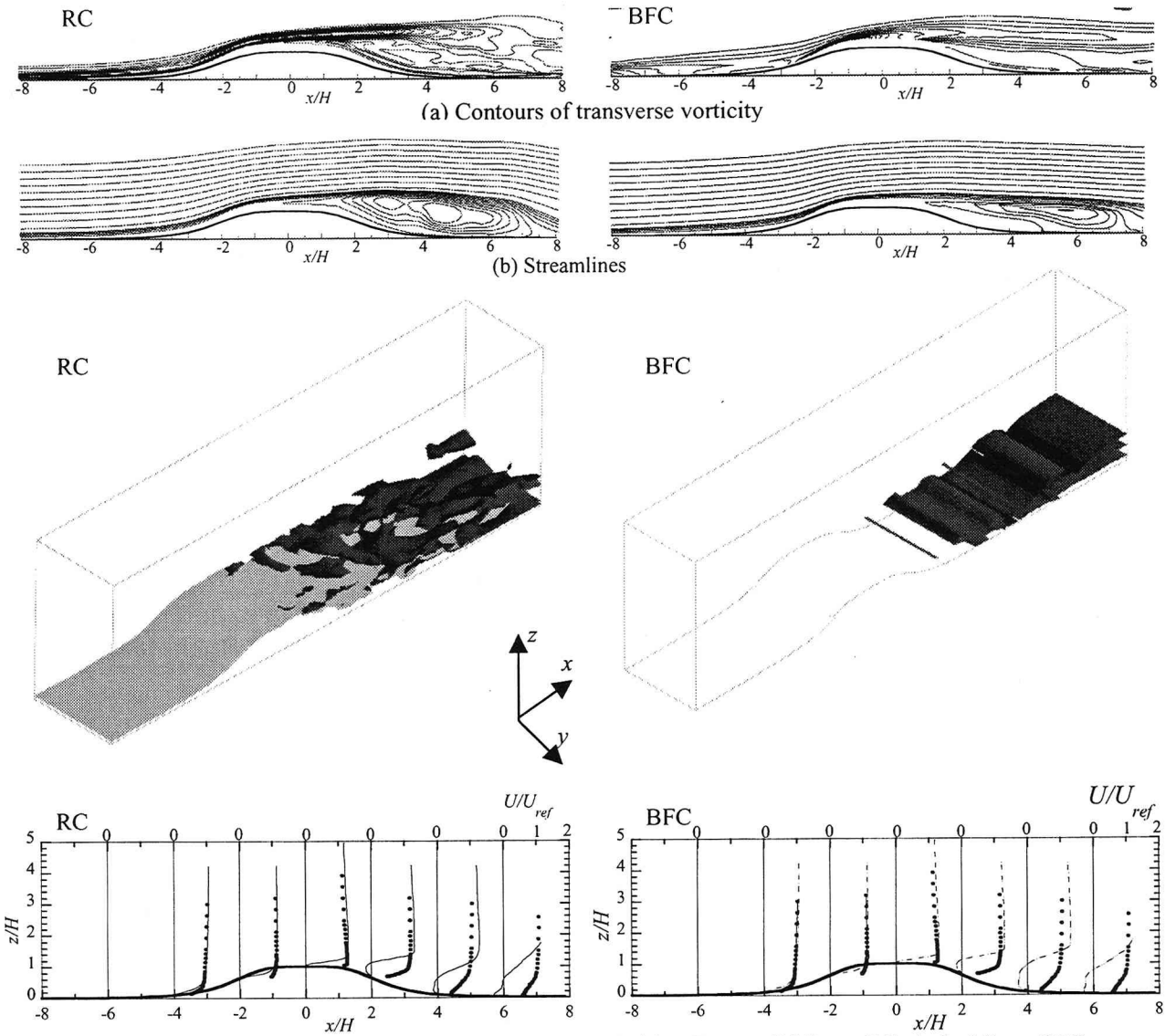

(d) Profiles of time averaged streamwise velocity; symbolds – Expt, solid line – RC, dashed line - BFC

Fig. 5. Calculation results for turbulent flow past hill of maximum slope of 25 degrees

of Miyashita[16]. Fig.4(a) presents a comparison of the transverse vorticity, and good agreement is seen. Streamlines obtained by RC and present BFC grids are compared in Fig.4(b) with those by Ref.16. Miyashita's calculation is two-dimensional and much denser grid of 260x70 is used and the numerical accuracy is considered to be better. Results agree very well although the recirculation flow is calculated slightly weaker in both RC and BFC. Fig.4(c) presents a comparison of the profiles of streamwise velocity component u/U_{ref} along several streamwise stations. The agreement is generally good as expected from the comparison of the streamlines. These mean that RC calculation with an appropriate upwind scheme produces good results

(2) Comparison in turbulent flow calculations

Flows in engineering and environmental applications are turbulent at much higher Reynolds numbers over more general boundary. We take the same geometry and examine the performance of the two methods of RC and BFC when applied in the LES calculation of turbulent flows. The flow at Reynolds number of 13000 has been measured[13] for maximum slope angle of 25 degrees. The mesh size is the same as that is used for laminar case. With this mesh, the first point from the ground near the top of hill is about 20 viscous units and hence the wall flow is not resolved. In such case, the wall model such as the wall function method is needed but in the present calculation, a straightforward no-slip condition is applied.

The velocity profile at the inflow plane of the calculation is adjusted such that it agrees with the experiment at x/H = -4. In the case of calculation using RC, computation using second-order conservative central differencing for convective terms diverged; hence, calculation is performed with UTOPIA scheme. BFC code is run with UTOPIA scheme too for comparison purpose. Calculation is run initially for 40,000 time steps before taking averages over the next 40,000 time steps.

The calculated mean-flow spanwise vorticity distribution and streamlines are compared in Fig.5 (a) and Fig.5(b). It is seen that the overall flow patterns calculated by both methods are similar. Small-scale disturbances, however are seen in the results of RC. These are considered to be due to the approximated boundary positions. In order to see the details of these disturbances, instantaneous streamwise vorticity distributions are shown in Fig.5(c). It shows that calculation by RC shows considerable three-dimensional features, but the BFC results do not. The profiles of time averaged velocity component U/U_{ref}, along specified streamwise stations computed using both rectangular and body-fitted grid and experimental results are plotted in Fig.5(d). At x/H=0 calculation shows the development of the boundary layer and the maximum velocity is drastically under-predicted. Both calculation results show a large recirculation region downstream of x/H=2, while experimental results show no separation. As explained before, the present calculation does not resolve the viscous sublayer. No wall model is used and the turbulence at the inflow plane does not exist. These are the reasons for not representing the boundary layer development correctly and not the grid representation. The main point is that in either grid system of representing the geometry, overall LES calculation results show the same trend.

7. CONCLUSIONS

Flow past curved hills has been computed by the numerical methods based on the boundary-fitted coordinate and the Cartesian coordinates to evaluate the merits and demerits of the two different approaches. Calculations are performed at low and high Reynolds number laminar flows to validate the numerical methods. While the calculation using central difference scheme for the convective terms leads to pressure oscillation when the geometry is approximated by rectangular grid, results are stable when the geometry is represented by a boundary-fitted grid or by using upwind scheme. At higher *Re* for turbulent flow condition, LES calculation results by with UTOPIA scheme for the convective terms shows similar trend in both grid systems. Hence, when calculation of flow past natural topography or complex geometry or open-channel flows with deforming free surfaces or impossible in generating BFC, is to be performed, rectangular coordinate approximation of the geometry with stability assured by upwind scheme for the convective terms is a good alternative and simulation by this method captures the flow features.

References

1) Mason, P.J: Large-eddy Simulation, A critical review of the technique, *Quarterly J. Roy. Meteorol. Soc*, 120, pp.117-162, 1994.

2) Nakayama, A. and Noda, H.: Physical and numerical modeling of turbulent flow over complex topography, *Proc. Turbulent Shear Flow*, 11, C19.19.1 – C19.19.6, 1997.

3) Verzicco, R., Mohd-Yosof, J., Orlandi, P. and Haworth, D.: Large eddy simulation in complex geometric configurations using boundary body forces, *AIAA, J.*, 38,3, pp.427-433, 2000.

4) Kitamura, S., Komurasaki, S. and Kuwahara, K.: Simulation of flow around a bluff body and the force, 14th *CFD Symposium*, Tokyo, B05-3, pp.60, 2000, (in Japanese).

5) Ichikawa, O. and Fujii, K.: 3D numerical simulation of flow field around arbitrary shape by using Cartesian grid, 14th *CFD Symposium*, Tokyo, E03-2, pp.175, 2000, (in Japanese).

6) Forrer, H. and Jeltsch, R.: A higher-order boundary treatment for Cartesian-grid methods, *J. Comput. Phys.*, 140, pp.259-277, 1998.

7) Ye, T., Mittal, R., Udayakumar, H. S. and Shyy, W.: An accurate Cartesian grid method for viscous incompressible flows with complex immersed boundaries, *J. Comput. Phys.*, 156, pp.209-240, 1999.

8) Morinishi, S., Lund, T., Vasilyev, O. V. and Moin, P.: Fully Conservative Higher Order Finite Difference Schemes for incompressible flow, *J.Comput.Physics*, 143, pp.90-124, 1998.

9) Nakayama, A. and Vengadesan, S. N.: On the simulation of numerical schemes and subgrid-stress models on LES of turbulent flow past a square cylinder, *Int. Jl. for Numerical methods in Fluids*, (to appear)

10) Nakayama, A. and Noda, H.: LES simulation of flow around a bluff body fitted with splitter plate, *J. Wind Eng. and Ind. Aerodyn.*, 85, pp.85-96, 2000.

11) Kajishima, T., Ohta, T., Okazaki, K. and Miyake, Y.: High-order finite difference method for incompressible flows using collocated grid system, *Transact. JSME B*, 63,614, pp.3247-3254, 1997, (in Japanese).

12) Yokojima, S. and Nakayama, A.: Development and verification of finite difference method based on collocated grid in generalized coordinate system for direct and large eddy simulations, *Annual J. Hydraulic Eng. JSCE*, 45, pp.565-570, 2001, (in Japanese).

13) Nakayama, A. and Yokota, D.: Experimental study of characteristics of rough surface boundary layer past gentle hills, *Annual J. Hydraulics Engg., JSCE*, 45, pp.43-48, 2001, (in Japanese).

14) Kogaki, T., Kobayashi, T. and Taniguchi, N.: Large eddy simulation of flow around rectangular cylinder, *Fluid Dynamics Research*, 20, pp.11-24, 1997.

15) Piomelli, U. and Balaras, E.: Numerical simulations using the immersed boundary technique, 3rd AFOSR *Inter. Conf. On DNS and LES*, Dallas, USA. pp.27, 2001.

16) Miyashita, K.: Simulation of turbulent flow over topography based on RANS method, Ph.D Thesis, Kobe University, 2001, (in Japanese).

(Received October 1, 2001)